Hindawi
Advances in Condensed Matter Physics
Volume 2018, Article ID 5731938, 7 pages
https://doi.org/10.1155/2018/5731938

Research Article

Numerical Simulations of Transfer of Spatial Beam Aberrations in Optical Parametric Chirped-Pulse Amplification

Ying Chen[1,2] **Yuan Zhou**[1] **Guobao Jiang**[1,2] **and Lulu Wang**[1]

[1] *School of Electronic Information and Electrical Engineering, Changsha University, Changsha, 410003, China*
[2] *Key Laboratory for Micro-/Nano-Optoelectronic Devices of Ministry of Education, School of Physics and Electronics, Hunan University, Changsha 410082, China*

Correspondence should be addressed to Guobao Jiang; andguobao@163.com and Lulu Wang; llw@ccsu.edu.cn

Received 21 June 2018; Accepted 30 August 2018; Published 1 October 2018

Academic Editor: Qinghua Guo

In this paper, the spatial characteristics of the optical parametric chirped-pulse amplification (OPCPA) process were numerically studied when initial pump beam was aberrated. Numerical results showed that the spatial walk-off effect transferred phase modulation partly to the signal beam as the pump phase was modulated. Moreover, the modulation amplitude became increasingly severe as the nonlinear length extended. In the absence of phase aberration in the initial input signal, the induced phase aberration in the output signal was assumed as the differential form of the pump beam phase. As the pump beam intensity was modulated, the spatial walk-off effect reduced the influence of pump beam noise on beam quality and the angular spectrum but reduced signal gain simultaneously; thus, it may do more harm than good in the OPCPA process. In the case of a non-diffraction-limited pump beam, the greater the beam quality factor M_p^2, the lower the conversion efficiency of the output signal in the OPCPA process. These results have important guiding significance for optimized design of an OPCPA system for high power laser.

1. Introduction

High-energy ultrashort solid lasers have comprised a development trend in laser optics in recent decades. In 1986, Strikland et al. suggested the idea of chirped-pulse amplification (CPA) [1], which dramatically reduced the possibility of nonlinear damage to the laser medium and fully leverages gain bandwidth during amplification [2, 3]. Optical parametric amplification (OPA) is an efficient approach of generating tunable pulses from a fixed laser source [4–6], including large energy fiber laser sources [7, 8]. The integration of OPA and CPA into optical parametric chirped-pulse amplification (OPCPA) has rapidly extended the peak power of amplified ultra-short laser pulses to the petawatt level due to unique features of efficient conversion, high gain, and broad bandwidth [9–13].

In strong-field physics applications, laser beam quality and pulse contrast are key issues in OPCPA laser systems [14]. To date, the pulse contrast of OPCPA systems has been studied extensively [15, 16], and various methods have been proposed to increase pulse contrast on a picosecond timescale [17–20]. However, less attention has been paid to beam quality in the OPCPA process, as the OPCPA technique was normally considered capable of ensuring the optical quality of an amplified signal field [16, 21]. This might not be a problem for most low-energy OPCPA systems where the pump laser sources are diffraction-limited or in a type 0 ($e_p \longrightarrow e_s + e_i$) quasi-phase-matching OPA process without spatial walk-off between interacting waves [22, 23]. However, circumstances are quite different for high-energy OPCPA systems where high-energy pump lasers are typically far below the diffraction limit [24, 25]. Meanwhile, the spatial walk-off effect is always present due to the adoption of birefringent nonlinear crystals.

Several articles have considered beam quality in OPCPA systems [26, 27], mainly by examining the influences of the pump beam-profile and dephasing on OPA gain and signal beam quality. A theoretical model was developed for dephasing effects due to angular deviation from ideal phase matching, and the impact of the angular content of

the beam on small signal gain and conversion efficiency in a strongly depleted regime was evaluated numerically [26]. In this paper, the spatial characteristics of the OPCPA process pumped by a spatially aberrated beam are studied theoretically and numerically. Three typical types of spatially aberrated pump beams are discussed, including the phase-modulated pump beam, intensity-modulated pump beam, and non-diffraction-limited pump beam. In the spatial domain, the nonlinear process of OPCPA is identical to that of OPA; thus, most parts of this paper do not differentiate explicitly between OPA and OPCPA.

2. Numerical Model

In this paper, the type I phase-matching OPA process is simulated by nonlinear coupled-wave equations in the spatial domain, implying that all temporal effects in the time domain are ignored. The equations governing the evolution of the envelopes E_p, E_s, and E_i of the pump, signal, and idler pulses [28, 29], respectively, are

$$\frac{\partial E_s(z,x)}{\partial z} + \frac{L_{NL}}{L_{sp}}\frac{\partial E_s(z,x)}{\partial x} + i\frac{L_{NL}}{L_{2s}}\frac{\partial^2 E_s(z,x)}{\partial^2 x} = -i\frac{\lambda_p}{\lambda_s}E_p(z,x)\,E_i^*(z,x)\,e^{-i\Delta kz} \quad (1)$$

$$\frac{\partial E_i(z,x)}{\partial z} + \frac{L_{NL}}{L_{ip}}\frac{\partial E_i(z,x)}{\partial x} + i\frac{L_{NL}}{L_{2i}}\frac{\partial^2 E_i(z,x)}{\partial^2 x} = -i\frac{\lambda_p}{\lambda_i}E_p(z,x)\,E_s^*(z,x)\,e^{-i\Delta kz} \quad (2)$$

$$\frac{\partial E_p(z,x)}{\partial z} + i\frac{L_{NL}}{L_{2p}}\frac{\partial^2 E_p(z,x)}{\partial^2 x} = -iE_s(z,x)\,E_i(z,x)\,e^{i\Delta kz} \quad (3)$$

where $E_j(z, x)$ is normalized to the input pump field E_0. For the sake of simplicity, a one-dimensional transverse model is used in simulations; diffraction effects are ignored due to the large beam aperture. A Gaussian pump beam is assumed throughout the paper, although different beam shapes may be involved. The spatial variable x is normalized to the radius of the pump beam waist w; $\Delta k = k_s + k_i - k_p$ is the wave-vector mismatch among the three waves, where wave vector $k_j = n\omega_j/c$. The nonlinear length is defined by $L_{NL} = n\lambda_p/(\pi\chi^{(2)}E_0)$ as a measure of the pump intensity. The pump beam is considered as the reference beam, thus, walk-off terms only appear in (1) and (2). The signal walk-off length L_{sp} is defined as $L_{sp} = w/\rho$, where ρ is the walk-off angle, and $L_{ip} = L_{sp}$ in the type-I collinear configuration. The ratio of L_{sp} to crystal length L indicates the practical walk-off magnitude of the OPA process in the nonlinear crystal. In the calculations, the initial signal wave is assumed to be a Gaussian beam with phase uniformity, and Δk is set to zero because it primarily affects signal gain and conversion efficiency, which has been thoroughly discussed [22]. Investigation of the walk-off effect in isolation can explicitly clarify its impact on the output signal beam. The standard split-step method and Runge-Kutta algorithm were adopted to solve the nonlinear equations numerically [29–31].

3. Analyses and Discussions

3.1. Pump Beam with Phase Modulation. First, the OPCPA process pumped by a phase-modulated beam is investigated. For simplicity, the pump beam is assumed to include sinusoidal phase modulation as $E(x,0) = E_0\exp(-x^2 + i\,a\sin^2(n\pi x))$, where parameters a and n correspond to the modulation amplitude and spatial frequency, respectively. The angular spectrum distributions of the signal beam and idler beam are displayed in Figure 1 under small-signal conditions. The insets in the top right corner are the local enlarged figure. As shown in Figure 1, the angular spectrum of the signal beam remain basically unchanged as the walk-off effect is not considered (the dotted line in Figure 1(a)). The phase modulation of the pump beam leads to angular spectrum aberration of the idler beam (the dotted line in Figure 1(b)). However, the angular spectrum of the signal beam become aberrated as the spatial walk-off effect is taken into account (the solid and dashed lines in Figure 1(a)). Additionally, the greater parameter a, the worse the angular spectrum aberration in the output signal beam, and the aberration of the idler beam is weakened accordingly. With regard to saturation amplification, the spatial characteristics of OPA are similar to those of the small signal.

Figure 2 shows the transverse distribution of the signal phase and its evolution in the crystal. As the pump phase is modulated by a sinusoidal phase, a sinusoidally modulated phase is observed in the output signal. The modulation amplitude increases in line with crystal length, as explained when analyzing the phase transfer mechanism of OPA. On account of spatial walk-off, the pump beam and idler beam are staggered in space, and their phases deviate. Their phase differences therefore become disordered, and the signal beam will partially undertake the distortion originated from the pump beam. Meanwhile, the greater the crystal length (or nonlinear length), the clearer the walk-off of the pump beam and idler beam. Moreover, the modulated amplitude of the signal phase became increasingly intense (see the phase curve in the position of z = 5 mm). One consequence of phase modulation is angular spectrum aberration, which also describes the phenomenon in the insets of Figure 1.

Figures 1 and 2 illustrate that the output signal inherited the aberration of the pump beam as its phase is modulated in the presence of spatial walk-off. Therefore, high-frequency modulation in the pump phase should be suppressed as much as possible to obtain a good-quality signal beam in the OPA process.

Figure 3 depicts the phase of the output signal when the pump phase $\Phi(x)$ is equal to x^2 and x^3, respectively. The shape in Figure 3(a) is approximately linear, whereas that in Figure 3(b) is approximately parabolic. Therefore, the induced phase of the signal is essentially the differential of the pump phase.

Next, the physical process of OPA is analyzed to explain the above phenomena. The phases of the signal (Φ_s), pump

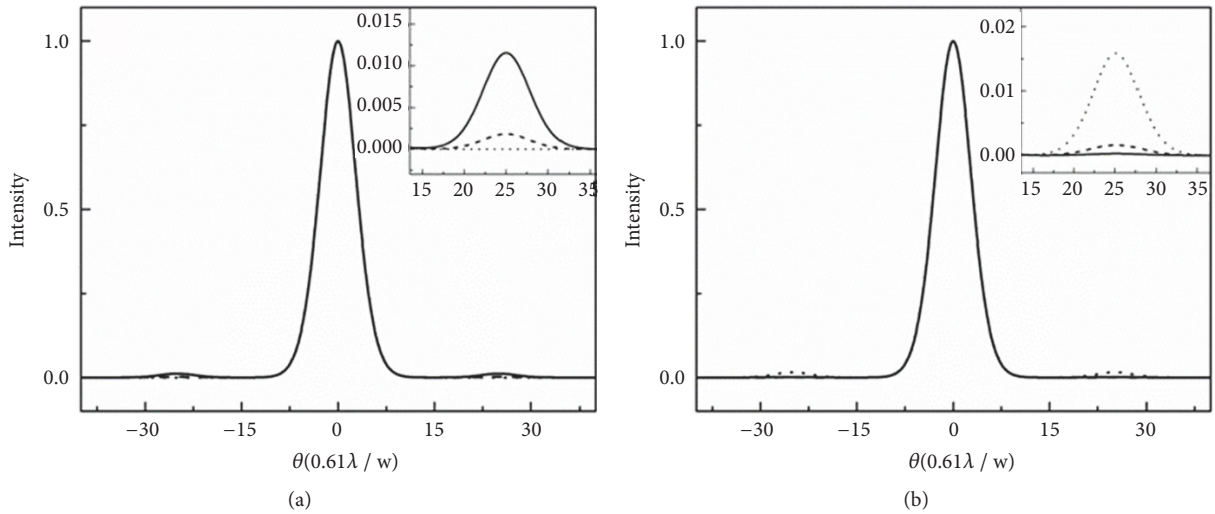

Figure 1: Angular spectrum of output signal beam (a) and idler beam (b) when pump phase is modulated. Dotted line: spatial walk-off effect not considered, $a = 0.5$. Dashed (solid) line: spatial walk-off effect considered, $a = 0.2$ (0.5). $E_0 = 10^{-6}$ (small-signal condition); crystal length L is 10 mm; $L_{NL} = 0.23L$; $L_{sp} = 5L$; $n = 4$.

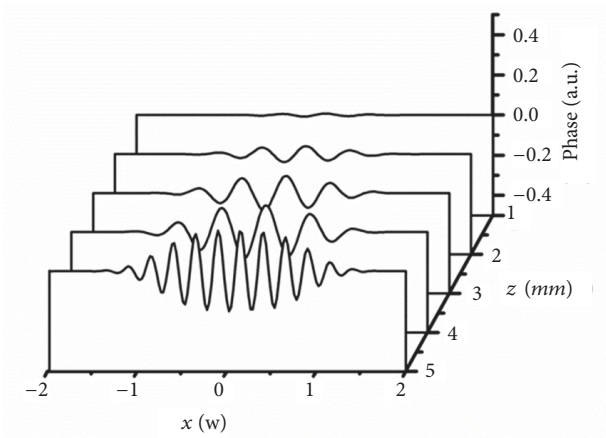

Figure 2: Evolution of signal phase in the transverse direction of nonlinear crystal under saturation amplification conditions ($E_0 = 10^{-2}$; $L_{NL} = 0.23L$, $L_{sp} = 5L$, $a = 0.5$, $n = 4$, $L = 5$ mm).

(Φ_p), and idler (Φ_i) are known to be fulfilled by the following relationship without walk-off effect and when the phase-matching condition is satisfied:

$$\Phi_s = \Phi_s(0) \tag{4}$$

$$\Phi_i = \frac{\pi}{2} + \Phi_p - \Phi_s \tag{5}$$

Equations (4) and (5) show that the phase of the output signal is independent of the pump phase, whereas the phase of the idler beam is related to the difference between Φ_s and Φ_p as the walk-off effect is neglected. Therefore, phase aberration in the pump beam will be transferred to the idler beam as the walk-off effect is ignored, as demonstrated by the dotted line in Figure 1(b). Supposing the phase of the initial signal is uniform, then the idler phase is consistent with that of the pump beam, denoted as $\Phi_p(x)+\pi/2$ and $\Phi_p(x)$, respectively. However, the pump beam and idler beam will no longer coincide in space if the walk-off effect occurs, resulting in some offsets. Similarly, if their phases are assumed to be $\Phi_p(x)$ and $\pi/2+\Phi_p(x+\Delta x)$, respectively, then the phase expression of the generated signal is $\Phi_s=\pi/2+\Phi_p(x)-(\pi/2+\Phi_p(x+\Delta x))=\Phi_p(x)-\Phi_p(x+\Delta x)$, representing the differential form of the pump phase and explaining the phenomena in Figure 3. The above theoretical results are helpful in precompensating or prefiltering phase aberration during the pulse-shaping process.

3.2. Pump Beam with Intensity Modulation. The spatial characteristics of the output signal are then analyzed as the pump amplitude is modulated. Given the amplified spontaneous emission, the pump beam usually generates noise. Therefore, it is necessary to discuss the effect of pump noise on the beam quality of the output signal.

The intensity modulation of the pump beam (namely the noise expression) is assumed to be $0.1E_0\sin^2(4\pi x)$, and the near-field distribution and angular spectrum of the output signal is obtained by numerical calculation as shown in Figures 4(a) and 4(b), respectively. Figure 4(a) indicates that the disturbance of the pump beam could be partially transferred to the signal beam, and the degree of noise transfer is weakened when the spatial walk-off effect is considered (the solid line in Figure 4(a)). The OPA gain is known to be related to pump intensity; therefore, the output signal is highly sensitive to the disturbance of pump intensity. When considering the walk-off effect, the sidelobes of the pump spectrum caused by its intensity modulation are not met the phase-matching condition, and these spatial frequency components are accordingly suppressed during the OPA process. Therefore, the beam quality of the output signal is somewhat better than that without walk-off effect. However, the gain of the signal beam clearly declines, as confirmed by the numerical simulation. The spatial walk-off effect is therefore

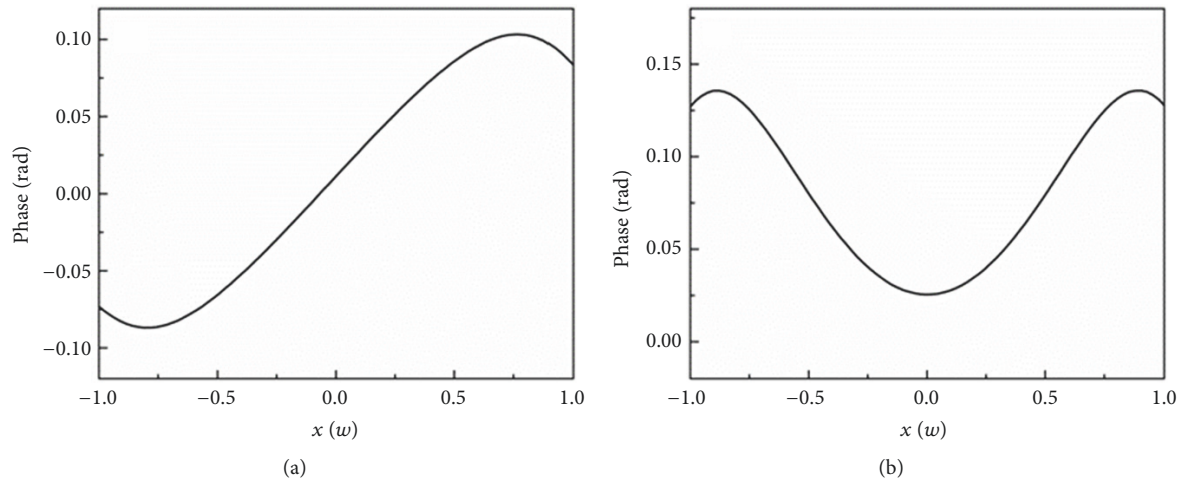

FIGURE 3: Phase curve of output signal when pump phase $\Phi(x)$ equals x^2 (a) and x^3 (b) ($L_{sp} = 5L$, $L_{NL} = 0.23L$, $L = 10$ mm, $E_0 = 10^{-6}$).

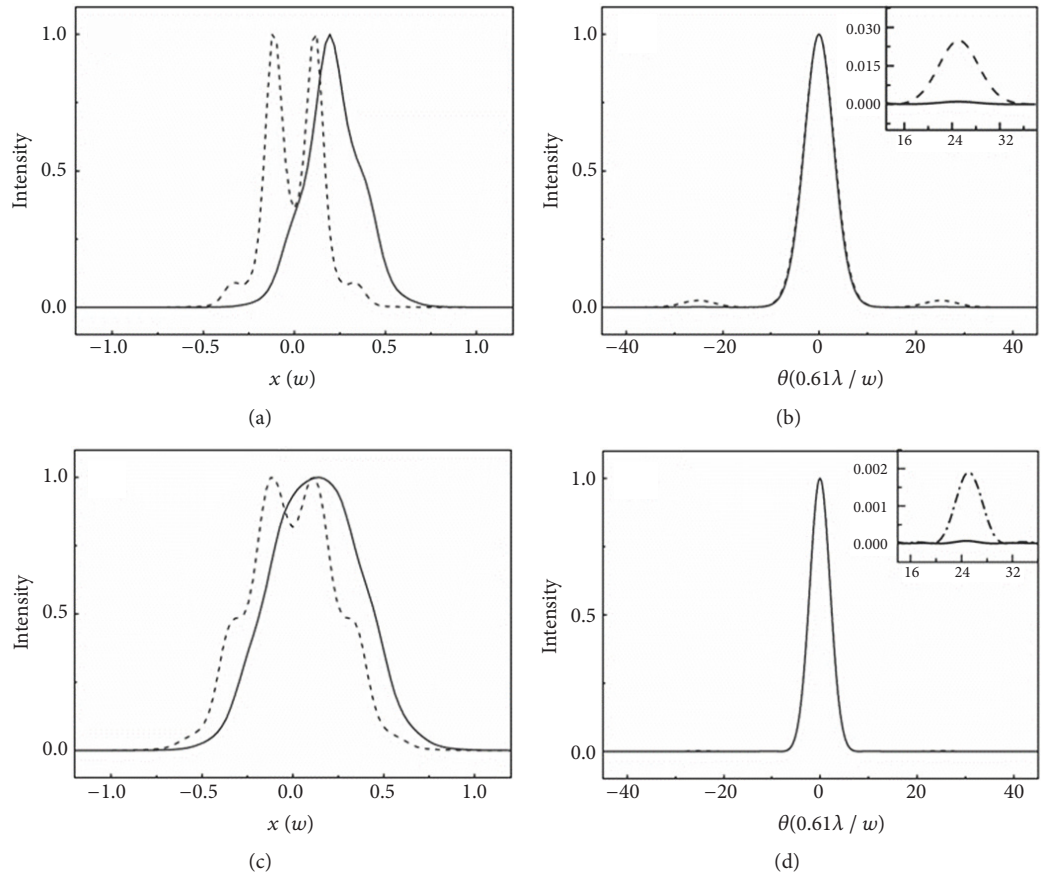

FIGURE 4: Near-field distribution (a, c) and angular spectrum (b, d) of the output signal when pump amplitude is modulated. Solid line: walk-off effect considered. Dashed line: no walk-off effect. (a) and (c) are stimulated under small-signal conditions ($E_0 = 10^{-6}$, $L = 10$ mm). (b) and (d) are calculated under saturation amplification conditions ($E_0 = 10^{-2}$, $L = 5$ mm). Other parameters are the same as those in Figure 1.

found to reduce the influence of pump noise on the near-field distribution and angular spectrum of the signal beam, which appears to benefit the OPA process. However, it also reduces the gain of the signal beam, which is not desirable. Therefore, the pump noise does more harm than good to the OPA process. In addition, the degree of fluctuation in the signal beam during saturation amplification (the dashed line in Figure 4(c)) is lower than the performance under small-signal conditions (the dashed line in Figure 4(a)), as the gain is more stable during the saturation amplification process.

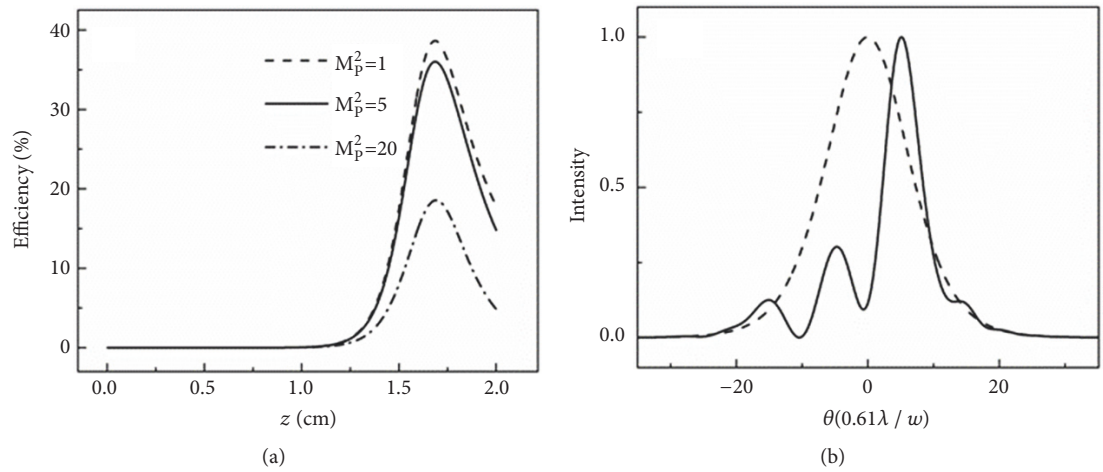

FIGURE 5: (a) Relationship between the signal gain and crystal length under different M_p^2 factors; (b) angular spectrum of pump beam (solid line) as the signal gain reaches the peak value; the dashed line is the initial angular spectrum of input pump beam, where $M_p^2 = 5$, $L_{NL} = 0.1L$, $L_{sp} = 5L$, $L = 20$ mm, $E_0 = 10^{-6}$.

3.3. Pump Beam Is Non-Diffraction-Limited. In this section, the influence of pump beam equality on signal gain is discussed as the pump beam is non-diffraction-limited. The pump beam is assumed to be a one-dimensional Gaussian beam with a slow varying phase, $E_p(0, x) = E_0 \exp[-x^2 + i\Phi(x)]$, where $\Phi(x) = \alpha \exp[-(x/2.5)^2] + \beta \exp[-(x/2.5)^4]$ and a and b are constants. From the perspective of beam quality, this expression describes the characteristics of typical high power lasers after spatial filtering [32]. Three pump beams are considered in this study, namely, $\alpha = 0$, $\beta = 0$; $\alpha = 94.0$, $\beta = 94.7$; and $\alpha = 177.0$, $\beta = 174.7$, with corresponding beam quality factors M_p^2 of 1, 5, and 20.

Figure 5(a) shows the relationship between signal gain and crystal length under different M_p^2 factors. The entire process of small-signal amplification, saturation amplification, and back conversion are numerically simulated. The signal gain is nearly zero within a large length (z<10 mm) at first in the case of small-signal amplification; it then rises rapidly, indicating saturation amplification, and finally decreases rapidly after reaching the peak, denoting a backconversion process. In addition, the shapes of the gain curves are similar under different M_p^2 factors, and the crystal lengths at which the signal gain reaches the peak value are almost the same. The only difference is that a larger M_p^2 factor leads to a lower signal gain peak. The formation of the three processes is related to energy consumption of the pump beam, and the signal gain originates from the pump energy. Initially, no pump energy loss occurs under small-signal amplification. Then, in the saturation amplification process, pump energy is quickly consumed. As the signal gain peaks, the pump energy is mostly consumed, as shown by the solid line in Figure 5(b). Next, some frequency components do not satisfy the phase-matching condition due to the spatial walk-off effect, and backconversion hence occurs with an increase in crystal length. The greater M_p^2 factor is, the more the frequency components fail not to satisfy the phase-matching condition, which is analogous to a reduction in pump intensity. As signal gain is closely related to pump intensity, the peak value of signal gain under the pump beam with a large M_p^2 factor is small, as shown by the dashed line in Figure 5(a). In addition, the divergence of the pump beam is assumed to be centrosymmetric, so the gain curves are similar under different M_p^2 factors. The poorer the pump beam quality is, the lower the signal gain is. Therefore, the quality of the pump beam should be optimized to minimize divergence or convergence before initiating the OPA process.

4. Conclusions

The spatial characteristics of the OPCPA process were analyzed in detail. In the numerical simulation, some effects were considered such as the walk-off effect, phase modulation, amplitude modulation of the pump beam, and pump beam quality. The walk-off effect was found to worsen signal beam quality in the OPCPA system when the pump beam exhibited phase modulation. However, as the pump intensity was modulated, the walk-off effect filtered out some aberrations; the signal beam quality improved but at the cost of reduced gain. In addition, the divergence or convergence of pump beam also compromised OPCPA gain. Therefore, it is highly important to select appropriate system parameters when designing the OPCPA system, such as a minimum walk-off angle, suitable crystal length, and good pump beam quality.

Data Availability

Figure 1 is the angular spectrum of output signal beam and idler beam as the pump phase is modulated. Figure 2 is the evolution of signal phase in the transverse direction of nonlinear crystal. Figure 3 is the phase curve of output signal as pump phase Φ(x) equals x2 and x3. Figure 4 is the near field distribution and the angular spectrum of the output signal as the pump amplitude is modulated. Figure 5(a) is the

relationship between the signal gain and crystal length under different factors; Figure 5(b) is the angular spectrum of pump beam. The experimental data used to support the findings of this study are all included within the article.

Conflicts of Interest

The authors declare that they have no conflicts of interest.

Acknowledgments

This work was partially supported the Natural Science Foundation of Hunan Province, China (Grant nos. 2018JJ2455 and 2018JJ3560), the Scientific Research Fund of Hunan Provincial Education Department (Grant nos. 16B026 and 17A020), and the Natural Science Foundation of China (Grant no. 61308005). The authors thank Yunfei Mo for enlightening discussions.

References

[1] D. Strickland and G. Mourou, "Compression of amplified chirped optical pulses," *Optics Communications*, vol. 55, no. 6, pp. 447–449, 1985.

[2] P. Maine, D. Strickland, P. Bado, M. Pessot, and G. Mourou, "Generation of Ultrahigh Peak Power Pulses by Chirped Pulse Amplification," *IEEE Journal of Quantum Electronics*, vol. 24, no. 2, pp. 398–403, 1988.

[3] M. D. Perry and G. Mourou, "Terawatt to petawatt subpico second lasers," *Science*, vol. 264, no. 5161, pp. 917–924, 1994.

[4] D. K. Negus, M. K. Steinershepard, M. S. Armas et al., "Micro joule-energy ultrafast optical parametric amplifiers," *Journal of the Optical Society of America B*, vol. 12, no. 11, pp. 2229–2236, 1995.

[5] G. Cerullo and S. De Silvestri, "Ultrafast optical parametric amplifiers," *Review of Scientific Instruments*, vol. 74, no. 1 I, pp. 1–18, 2003.

[6] G. Andriukaitis, T. Balčiunas, S. Ališauskas et al., "90 GW peak power few-cycle mid-Infrared pulses from an optical parametric amplifier," *Optics Expresss*, vol. 36, no. 15, pp. 2755–2757, 2011.

[7] Y. Chen, C. Zhao, S. Chen et al., "Large Energy, Wavelength Widely Tunable, Topological Insulator Q-Switched Erbium-Doped Fiber Laser," *IEEE Journal of Selected Topics in Quantum Electronics*, vol. 20, no. 5, pp. 315–322, 2014.

[8] S. Lu, C. Zhao, Y. Zou et al., "Third order nonlinear optical property of Bi2Se3," *Optics Express*, vol. 21, no. 2, pp. 2072–2082, 2013.

[9] I. N. Ross, P. Matousek, M. Towrie et al., "The prospects for ultrashort durationand ultrahigh intensity using optical parameteric chirped pulse amplifications," *Optics Communications*, vol. 144, no. 1, pp. 125–133, 1997.

[10] L. Cai, J. H. Wen, D. L. Yu et al., "Design of the coordinate transformation function for cylindrical acoustic cliaks with a quatity of discrete layers," *Chinese Physics Letter*, vol. 31, no. 9, Article ID 030201, 2014.

[11] L. Yu, X. Liang, L. Xu et al., "Optimization for high-energy and high-efficiency broadband optical parametric chirped-pulse amplification in LBO near 800 nm," *Optics Letters*, vol. 40, no. 14, pp. 3412–3415, 2015.

[12] J. H. Sung, H. W. Lee, J. Y. Yoo et al., "4.2 PW, 20 fs Ti:sapphire laser at 0.1 Hz," *Optics Letters*, vol. 42, no. 11, pp. 2058–2061, 2017.

[13] X. Zeng, K. Zhou, Y. Zuo et al., "Multi-petawatt laser facility fully based on optical parametric chirped-pulse amplification," *Optics Expresss*, vol. 42, no. 10, pp. 2014–2017, 2017.

[14] R. A. Snavely, M. H. Key, S. P. Hatchett et al., "Intense high-energy proton beams from petawatt-laser irradiation of solids," *Physical Review Letters*, vol. 85, no. 14, pp. 2945–2948, 2000.

[15] H. Yoshida, E. Ishii, R. Kodama et al., "High-power and high-contrast optical parametric chirped pulse amplification in β-BaB2O4 crystal," *Optics Expresss*, vol. 28, no. 4, pp. 257–259, 2003.

[16] L. Cai, H. Xiaoyun, and W. Xisen, "Band-structure results for elastic waves interpreted with multiple-scattering theory," *Physical Review B*, vol. 74, no. 15, 2006.

[17] H. Ren, L. Qian, H. Zhu, D. Fan, and P. Yuan, "Pulse-contrast degradation due to pump phasemodulation in optical parametric chirped-pulse amplification system," *Optics Express*, vol. 18, no. 12, pp. 12948–12959, 2010.

[18] J. H. Sung, W. Y. Jin, J. Lee et al., "Generation of high-contrast, 30 fs, 1.5 PW laser pulses from chirped-pulse amplification Ti:sapphire laser," *Optics Express*, vol. 20, no. 10, pp. 10807–10815, 2012.

[19] V. Bagnoud and F. Wagner, "Ultrahigh temporal contrast performance of the PHELIX petawatt facility," *High Power Laser Science and Engineering*, vol. 4, no. 4, 2016.

[20] X. L. Wang, X. M. Lu, X. Y. Guo et al., "Experimental investigation on pulse-contrast degradation caused by surface reflection in optical parametric chirped-pulse amplification," *Chinese Optics Letters*, vol. 16, no. 5, 2018.

[21] I. N. Ross, P. Matousek, G. H. C. New, and K. Osvay, "Analysis and optimization of optical parametric chirped pulse amplification," *Journal of the Optical Society of America B*, vol. 19, no. 12, pp. 2945–2956, 2002.

[22] I. Jovanovic, J. R. Schmidt, and C. A. Ebbers, "Optical parametric chirped-pulse amplification in periodically poled KTiOPO4 at 1053 nm," *Applied Physics Letters*, vol. 83, no. 20, pp. 4125–4127, 2003.

[23] B. W. Mayer, C. R. Phillips, L. Gallmann, and U. Keller, "Mid-infrared pulse generation via achromatic quasi-phase-matched OPCPA," *Optics Express*, vol. 22, no. 17, pp. 20798–20808, 2014.

[24] T. Tajima and G. Mourou, "Zettawatt-exawatt lasers and their applications in ultrastrong-field physics," *Review of Modern Physics*, vol. 5, no. 3, pp. 419–426, 2001.

[25] O. V. Chekhlov, J. L. Collier, I. N. Ross et al., "35 J broadband femtosecond optical parametric chirpedpulse amplification system," *Optics Expresss*, vol. 31, no. 24, pp. 3665–3667, 2006.

[26] I. Jovanovic, B. J. Comaskey, and D. M. Pennington, "Angular effects and beam quality in optical parametric amplification," *Journal of Applied Physics*, vol. 90, no. 9, pp. 4328–4337, 2001.

[27] O. Novák, H. Turčičová, M. Divoký et al., "Mismatch characteristics of optical parametric chirped pulse amplification," *Laser Physics Letters*, vol. 11, no. 2, 2014.

[28] X. Wei, L. Qian, P. Yuan et al., "Optical parametric amplification pumped by a phase-aberrated beam," *Optics Express*, vol. 16, no. 12, pp. 8904–8915, 2008.

[29] L. L. Wang, Y. Chen, and G. C. Liu, "Increased temperature acceptance bandwidth in frequency doubling process using two different crystals," *Chinese Optics Letters*, vol. 12, no. 11, 2014.

[30] S. Chen, L. Miao, X. Chen et al., "Few-layer topological insulator for all-optical signal processing using the nonlinear kerr effect," *Advanced Optical Materials*, vol. 3, no. 3, pp. 1769–1778, 2016.

[31] S. Chen, Q. Wang, C. Zhao, Y. Li, H. Zhang, and S. Wen, "Stable single-longitudinal-mode fiber ring laser using topological insulator-based saturable absorber," *Journal of Lightwave Technology*, vol. 32, no. 22, pp. 3836–3842, 2014.

[32] T. Wang, T. Zhan, H. Zhu, and L. Qian, "Analysis of beam-quality degradation in nonlinear frequency conversion," *Journal of the Optical Society of America B*, vol. 19, no. 5, pp. 1101–1106, 2002.